MECHANICAL AND DIMENSIONAL CHARACTERISTICS OF FUSED DEPOSITION MODELING BUILD STYLES

Eric Fodran[⊕], Martin Koch[+], and Unny Menon[+]

⊕ MATERIALS ENGINEERING DEPARTMENT
+ INDUSTRIAL & MANUFACTURING ENGINEERING DEPARTMENT

CALIFORNIA POLYTECHNIC STATE UNIVERSITY
SAN LUIS OBISPO, CA 93407, USA

1.   Abstract

As rapid prototyping becomes more prominent, industry relies more on the mechanical properties of the builds. Fused Deposition Modeling (FDM) tensile samples were constructed and tested in order to characterize the mechanical properties of Acrylonitrile Butadiene Styrene (ABS) FDM builds. Parameters such as fill gap, line width, and slice thickness were varied in the production of the FDM samples. This was performed independently to isolate the effect of each parameter on mechanical properties. Results include the ultimate tensile strength, yield strength, elongation, energy to fracture, modulus of elasticity, and dimensional analysis. High magnification fracture surface analysis was also be performed to aid in the characterization of sample failures.

2.   Introduction

The mechanical properties of polymers are characterized in the same manner as metals using stress strain curves and the parameters derived from those curves. Polymer materials display the brittle and ductile behavior observed in metals as well as behaving in a highly elastic manner (Berns 1991).

All forms of mechanical stress have components of tensile loading. In bending, the layer of material on the outside of the bend radius is in tension. In shear, the material at $90°$ to the direction of shear is in tension. In torsion, the material on the entire circumference is in tension. Even in compression, there is a component of tensile loading through the center of the sample due to the elastic properties of plastics (Gere and Timoshenko 1990), (Berns 1991). Due to this wide influence of tensile strength, it is the most common property referred to when considering general strength of materials (Berns 1991).

There can be one or two phases during the failure of a polymer under tension. The material may first yield, which results in a reduction of its load carrying capacity, but continue to elongate. The second phase is "brittle and rapid failure" (Gere and Timoshenko 1990). Yielding occurs when the load to overcome the intermolecular secondary forces is less than that required to break primary molecular bonds. Within the yielding phenomena, the long chain-like molecules begin to uncoil and slip past each other. If the load persists, the material will continue to elongate with continued molecular orientation. Further loading results in considerable molecular orientation in which the molecules are almost completely aligned in an anisotropic fashion in the direction of loading. At this point the load begins to be resisted by primary molecular bonds. The load carrying capacity may then increase until the primary bond strength within the molecular chains is exceeded and the material undergoes rapid brittle failure (Berns 1991).

Accurate experimental results will depend on the load being distributed uniformly throughout the gage section. If the load distribution is non-uniform, the true length in which deformation occurs will not be known. In such cases, using the gage length in the calculations will produce erroneous values. Surface

defects and contamination are other common causes of erroneous tensile data. Nicks, scratches, bubbles, or other defects on the surface of test samples serve as an initiation site for fractures. As the test starts, stress builds uniformly throughout the gage section of the sample as the molecules distribute the stress evenly among themselves. The molecules bordering a surface defect cannot distribute the stress to the molecules on the other side of the defect (Courtney 1990).

If the defect arises from solid contamination, the adhesive attraction of the molecules to the defect is low. The stress is channeled from the molecules bordering the defect to the molecules located where the defect stops. Concentration of the stress occurs where the two sides of the defect meet at $90°$ to the direction of loading. The stress will increase rapidly at the concentration point and primary molecular bonds will break. A crack will develop which will then serve as a defect itself and will propagate through the material by the same action that initiated at the original defect.

Rate of deformation is another important factor in determining measurements obtained from testing. Stress in a sample is actually the polymer's response to deformation. A tensile testing machine pulls on a sample causing deformation. The resistance to the deformation is the value which is measured and used to calculate tensile properties. A high rate of deformation allows less time for molecules to mobilize and uncoil to locally relieve the stress. This results in less deformation before primary bonds are broken and potentially a lower stress value at failure. Significant reductions can also be seen in yield and ultimate elongation. To prevent such phenomena, sufficient cross head speeds are selected per tensile test.

After the proper testing parameters are obtained, tensile tests will be conducted in accordance to ASTM standard D 638 (Figure 1). All data which is obtained from testing will then be tabulated for interpretation.

3.   Fused Deposition Modeling

The polymer to be tested will be FDM constructed ABS. Fabrication of a FDM piece is a multi-step procedure. Using a computer, a three dimensional image is first sliced into cross-sectional planes. These planes are used by the Stratasys 1600 rapid prototyping machine to build the part, layer-by-layer (Figure 2). The first layer of the part is bonded by the FDM machine to a support platform via an extruded path defined by the shape of the first computer-sliced area. The FDM platform is lowered a preset distance after the first layer has been laid down. Material is then extruded over the surface of the first layer and bonded to form the second layer. The process repeats until the complete three dimensional structure is constructed.

Van Weeren et al (Weeren 1995) here examined the quality of FDM constructed pieces with respect to the defects in ceramic materials. Our investigations focus on ABS, the most widely used material for FDM manufacturing at this time. This study on the strength of ABS-FDM builds will

form the basis of future research on enhancing ABS-FDM RP parts by post processing with epoxies or other composite supplements to enhance strength for lower density ABS builds for FDM machines.

When a molten polymer is joined to a solid polymer, incomplete bonding can result. This can cause lower tensile strength along this bonding interface. Once the melt comes in contact with the solid, the bond looses its structural integrity along the surface of separation. This occurs because polymer molecules can only reestablish a high degree of interlinking across the surface by a slow diffusion process that is driven by thermal (Brownian) motion (Courtney 1990).

4.   Visual and Dimensional Analysis

In order to verify the builds produced by the FDM machine, Scanning Electron Microscopy was performed. At high magnification, parameters such as fill gap, line width, and slice thickness can be confirmed prior to actual testing of the samples (Figure 3). After testing of the samples is completed, SEM analysis can again be employed to characterize the failure of the specimens (Figure 4). Dimensional analysis was performed throughout experimentation (Figure 5). This analysis can thus verify the dimensional integrity of the FDM constructed builds.

5.   Experimental Results and Discussion

Initial experimentation was performed on samples which were constructed in accordance to three different build style parameters. The parameters for these build styles have been summarized in the following table:

Build Style Sample #	Layer Width	Raster Angle	Gap	Road Fill
1	0.010"	45°,45°	0	0.020"
2	0.010"	45°,45°	0	0.015"
3	0.010"	Contour	0	0.020"

Experimentation has yielded the following results:

Build Style/ Sample#	Peak Stress (MPa)	Fracture Stress (MPa)	Elongation at Fracture (mm)	Modulus (GPa)	Energy to Fracture (J)
1	17.33	15.51	0.851	0.961	0.125
2	19.42	16.81	1.21	1.02	0.21
3	21.15	17.23	1.04	1.08	0.18

This preliminary empirical data demonstrates the contour constructed specimens exhibit the strongest properties under such tensile forces. In the case of the contour constructed samples, the ABS lines in the necked gage section of the sample are all aligned in an anisotropic orientation in the axis of loading. Such orientation would then lead to quantify the resistance of the lines themselves, not the bond forces between them, as in the case of samples 1 and 2.

Further research was performed on enhancing ABS-FDM parts by post processing with several different epoxies and adhesives. The tensile specimens were constructed from the same design, altering only the gap between +45°/-45° rasters. The gaps selected for this experiment were 0.02", 0.03", and 0.05". Build parameters are summarized in the following table.

Build Style/Sample#	Layer Width	Raster Angle	Gap	Road Fill
1	0.010"	45°,45°	0	0.020"
2	0.010"	45°,45°	0	0.015"
3	0.010"	Contour	0	0.020"

Four bonding agents which were ABS compatible were selected and impregnated into tensile specimens by hand lay-up techniques. After proper cure time the specimens were tested in accordance to ASTM D 638. The following tables and charts summarize the results from the performed tensile tests:

Peak Tensile Stress (MPa) for Post-Processed Specimens

		Gap		
		0.02"	0.03"	0.05"
Adhesive	Baseline	10.58	7.12	10.87
	5Min	17.30	15.53	19.54
	MDGlue	16.18	15.49	19.08
	Clear	13.05	8.25	12.16
	Ultra	16.29	16.25	19.82

Tangent Modulus (MPa) for Post-Processed Specimens

		Gap		
		0.02	0.03	0.05
Adhesive	Baseline	0.43	0.28	0.42
	5Min	1.31	1.20	1.18
	MDGlue	0.85	0.86	0.85
	Clear	0.37	0.28	0.50
	Ultra	0.78	0.81	0.95

Peak Stress For All Samples

Legend: 0.02, 0.03, 0.05 (MPa vs Baseline, Clear, MDGlue, 5Min, Ultra)

Tangent Modulus For All Samples

Legend: 0.02, 0.03, 0.05 (MPa vs Baseline, Clear, MDGlue, Ultra, 5Min)

424
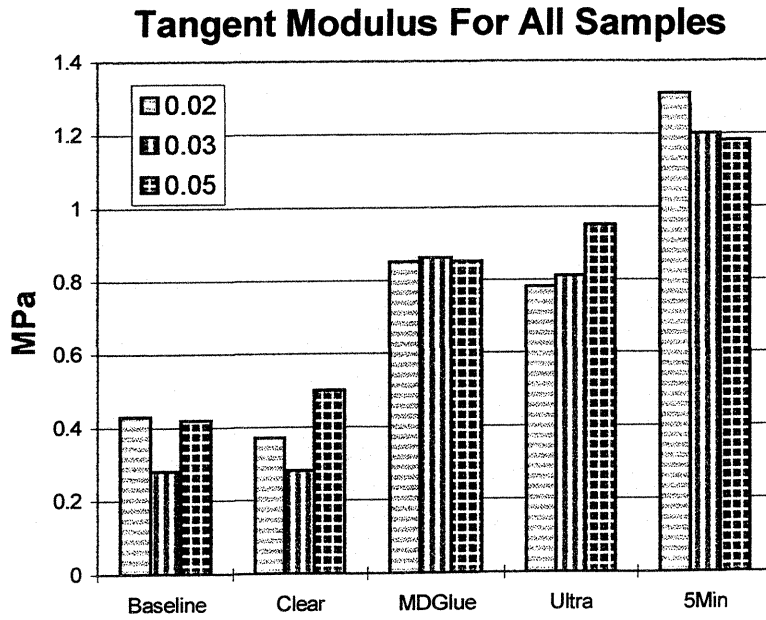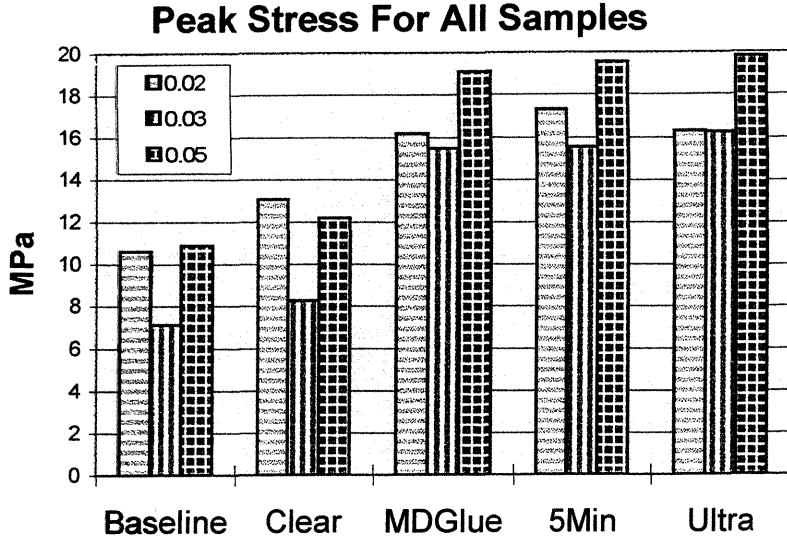
The data and graphical illustrations clearly illustrate an increase in the tensile strength of the specimens as a result of applying any of the bonding agents. The tangent modulus was also increased with the addition of the bonding agents in all but one of the four cases.

Photomicrographs obtained through scanning electron microscopy illustrate the surface topography of the fracture surface of the tensile specimens tested. Failure of the samples impregnated with the bonding agents have been characterized and placed into one of several categories. With the bonding agents acting as a matrix and the ABS polymer as a reinforcing/filler material, the fracture surfaces were categorized as exhibiting one of the following appearances: brittle matrix failure and ductile polymer failure, mutually ductile failure, and mutually brittle failure (Figures 6 -).

The fracture surface of the "MDGlue" adhesive demonstrated the highest degree of mutually ductile failure modes of all the samples analyzed in all build styles (Figures 6 - 12). Figure 12 at 580X clearly illustrates the similar ductile fracture surface of the matrix and fiber. Note also the mixed modes of adhesive and cohesive failure at the fiber matrix interface (Figure 7).

The fracture surface of the samples impregnated with the "Clear" adhesive also demonstrated a considerable degree of mutually ductile failure(Figures 13-16). In contrast to the samples impregnated with the "MDGlue" adhesive, the "Clear" samples exhibited all adhesive failure at the matrix/fiber interface without indication of any cohesive failure (Figures 13, 14).

Both the "5Min" and "Ultra" adhesives resulted in fracture surfaces which exhibited brittle failure of the matrix and ductile failure of the fibers (Figures 17 - 24 and Figures 25 - 32 respectively) In all of the figures for the two adhesives a definite lack in deformation prior to fracture is evident.

It has been determined that the mechanical properties of FDM modeled samples can be manipulated by the standard in which they are built. The properties can easily be altered by the modification of one of the criterion of FDM construction. In addition the mechanical properties can again be improved by the impregnation of common bonding agents. Not only can adhesive be selected to increase the mechanical properties, but also can also to control the mode of failure between the bonding agent and polymer fiber.

6.   Acknowledgments

7.   References

Michael L. Berns (1991) <u>Plastics Engineering Handbook of the Plastics Industry,</u> <u>5th Edition</u>, New York, Van Norstrand Reinhold.

Thomas H. Courtney (1990) <u>Mechanical Behavior of Materials</u>, New York, McGraw-Hill.

James M. Gere and Stephen P. Timoshenko (1990) <u>Mechanics of Materials, 3rd</u> <u>Edition</u>, New York, PWSKENT Publishing Co.

Weeren R. , Agarwala M. , Jamalabad V. R. , Bandyophadadyay A. , Vaidyanathan R. , Langrana N. , Safari A. , Whalen P. , Danforth S. C. , Ballard C. (1995) Quality of Parts Processed by Fused Deposition. **Solid Freeform Fabrication Conference Proceedings**, University of Texas, Austin, September 1995, pp 314-321.
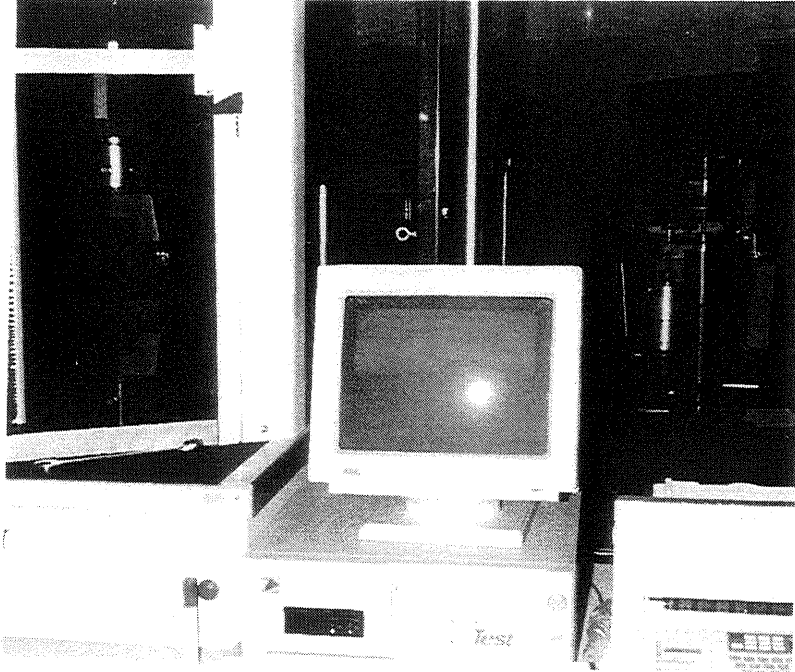
Figure 1: Tensile load frame with FDM constructed sample, approximate sample size ~80mm.

Figure 2: Stratasys 1600 FDM apparatus in process.
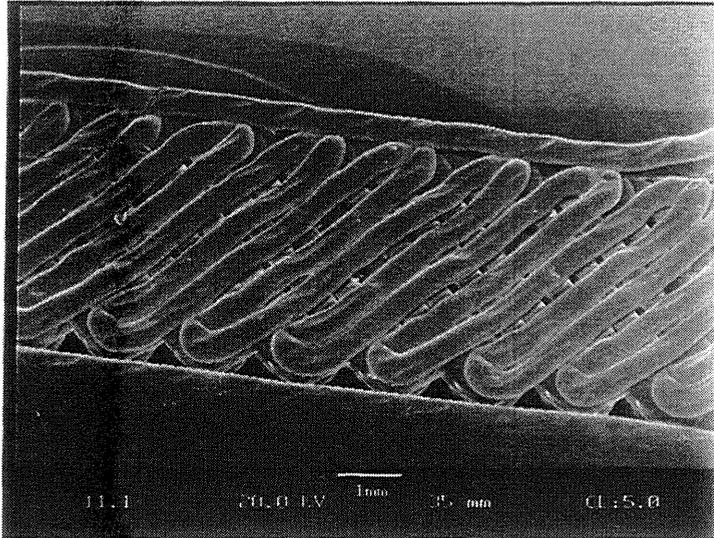
Figure 3: Surface roads and side view if slices.
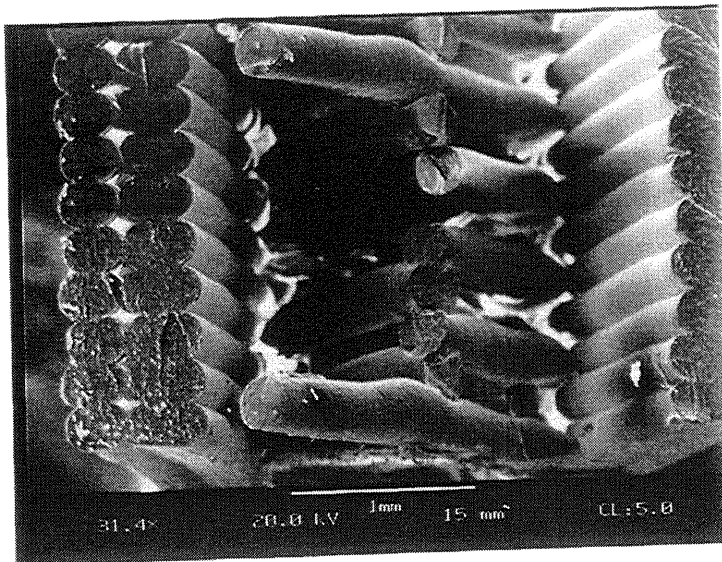
Figure 4: Fracture surface of FDM constructed ABS tensile sample.
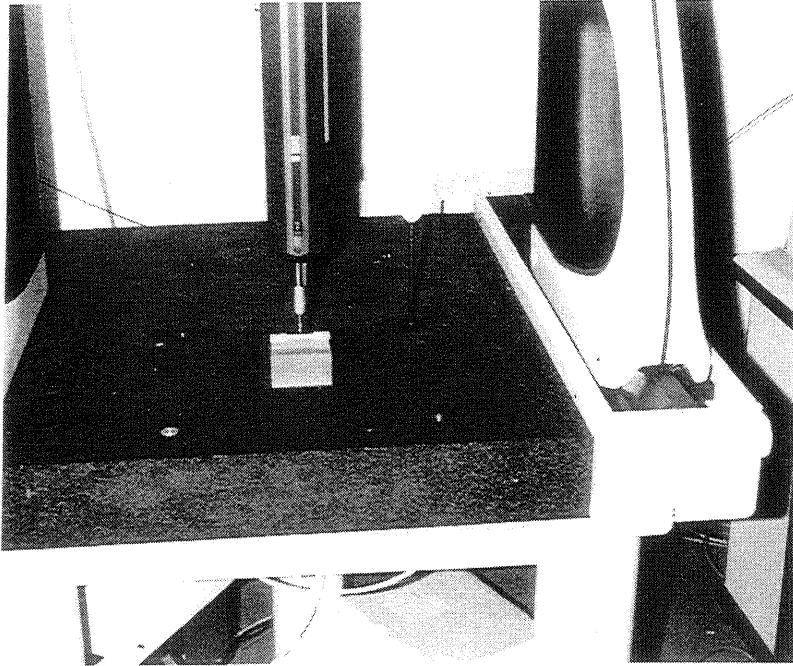
Figure 5: Dimensional analysis apparatus.
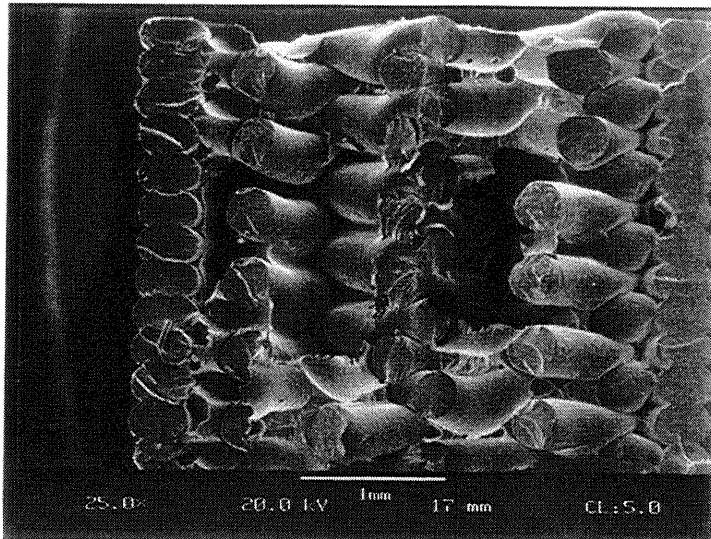
Figure 6: Fracture surface of MDGlue impregnated sample at 0.02" gap and 25X.
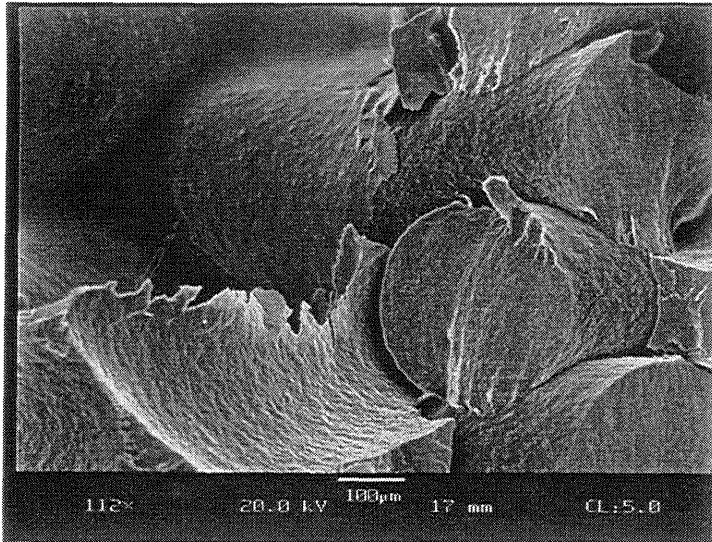
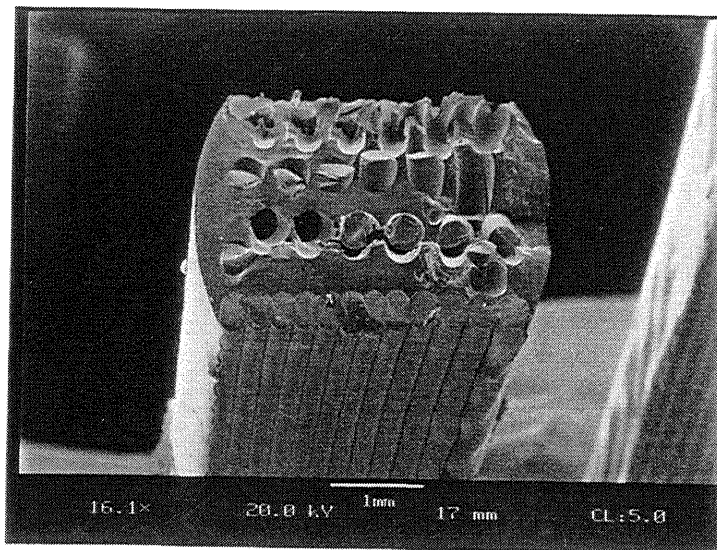Figure 7: Fracture surface of MDGlue impregnated sample at 0.02" gap and 112X.
Note the mixed cohesive and adhesive failure at the fiber/matrix interface.
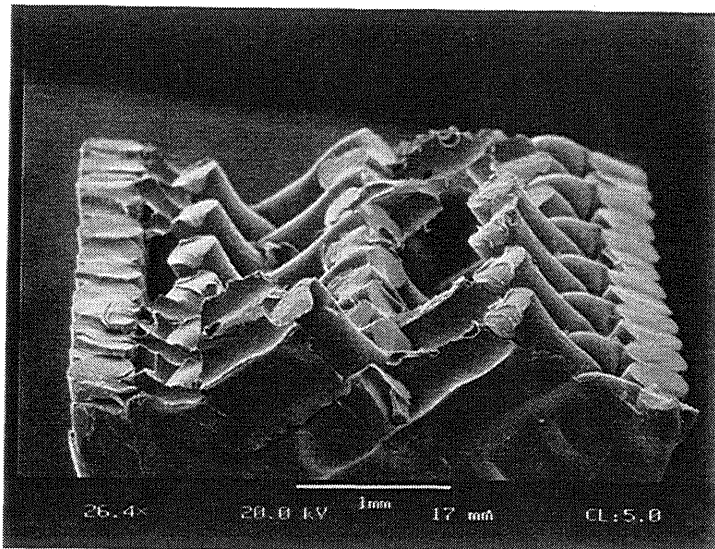
Figure 8: Fracture surface of MDGlue impregnated sample at 0.02" gap and 26.4X.
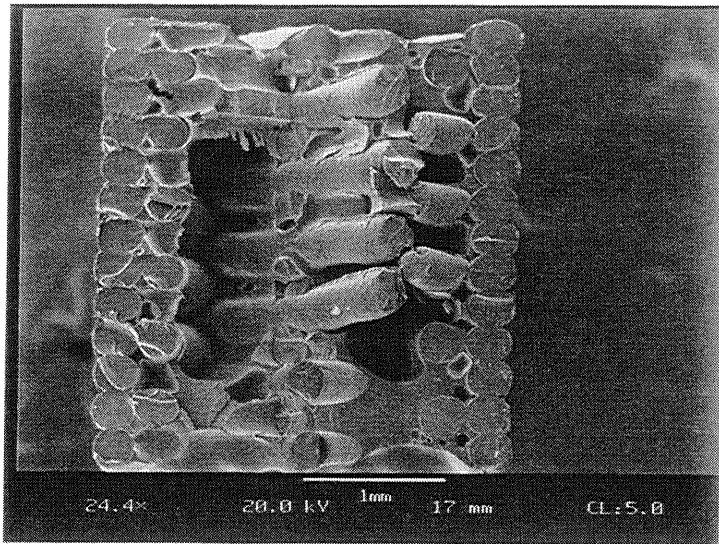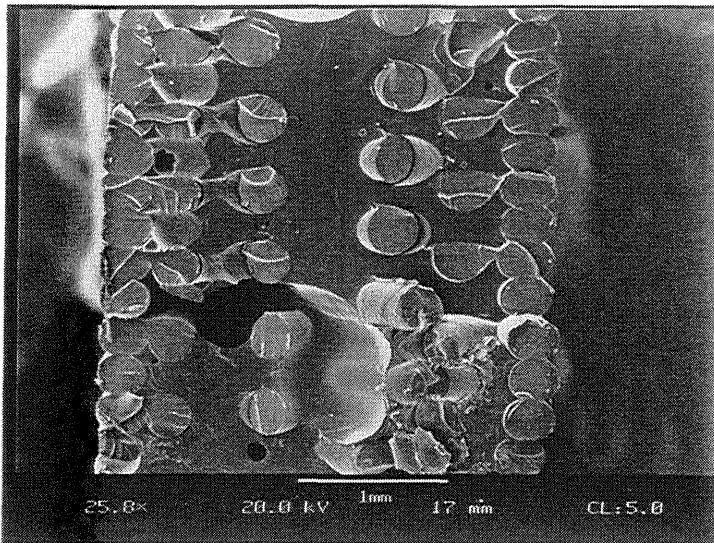
Figure 9: Fracture surface of MDGlue impregnated sample at 0.03" gap and 24.4X.
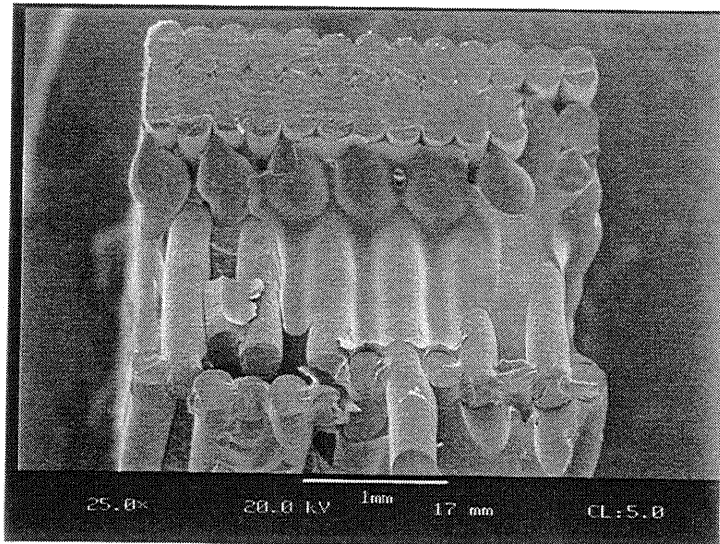
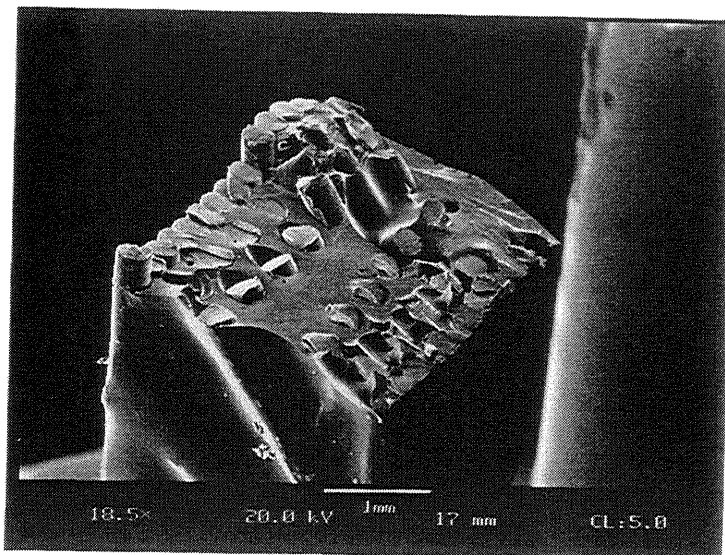

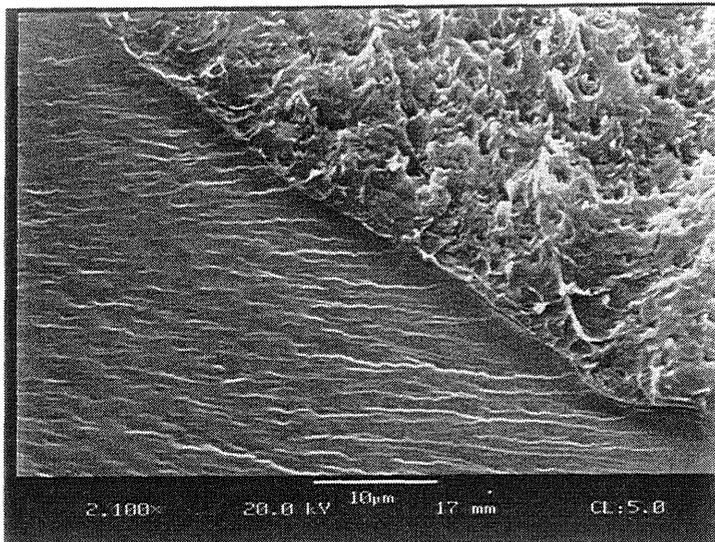Figure 10: Fracture surface of MDGlue impregnated sample at 0.05" gap and 25.8X.

431
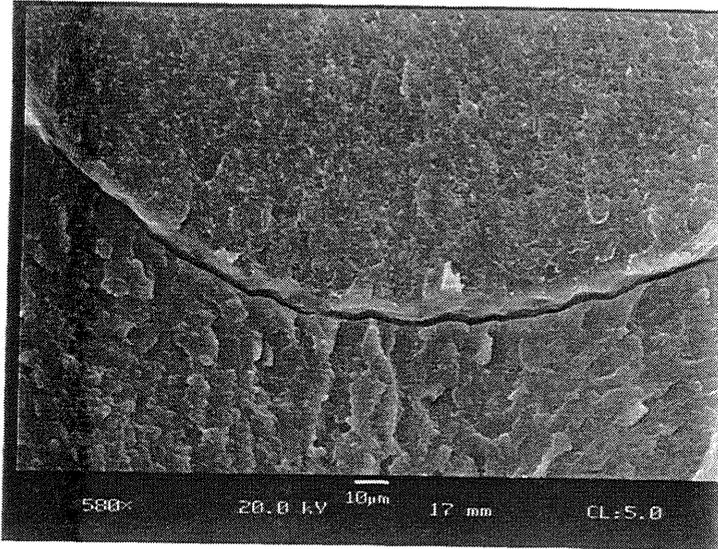
Figure 11: Fracture surface of MDGlue impregnated sample at 0.05" gap and 580X.
Note the similarity of the ductile appearance between the polymer fiber in the upper portion of the photomicrograph and the adhesive matrix in the lower.
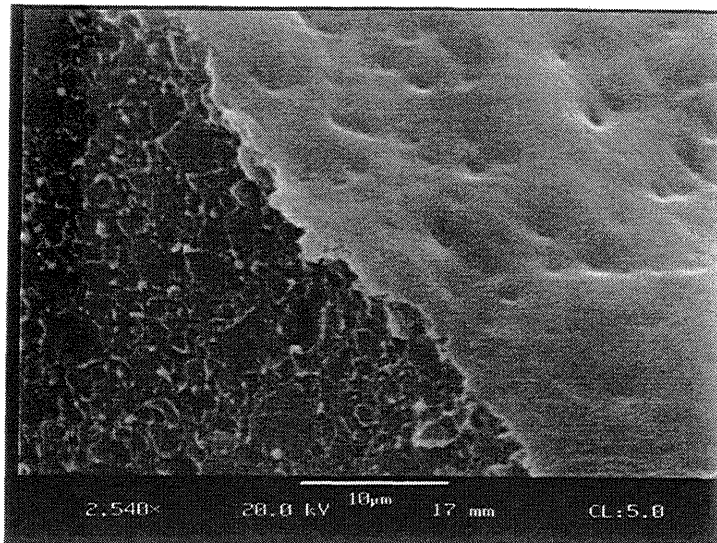
Figure 12: Fracture surface of MDGlue impregnated sample at 0.05" gap and 2540X.
The lower left portion of the photomicrographs illustrates the fracture surface of the adhesive at high magnification, while the upper right displays the adhesive fracture at the interface.
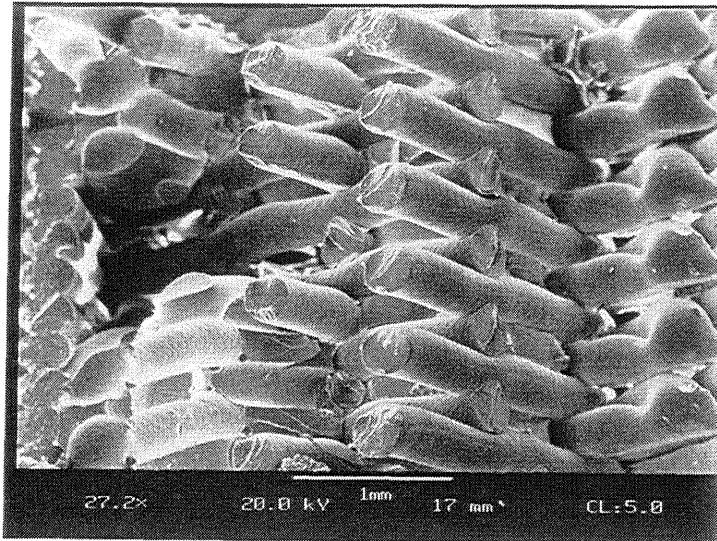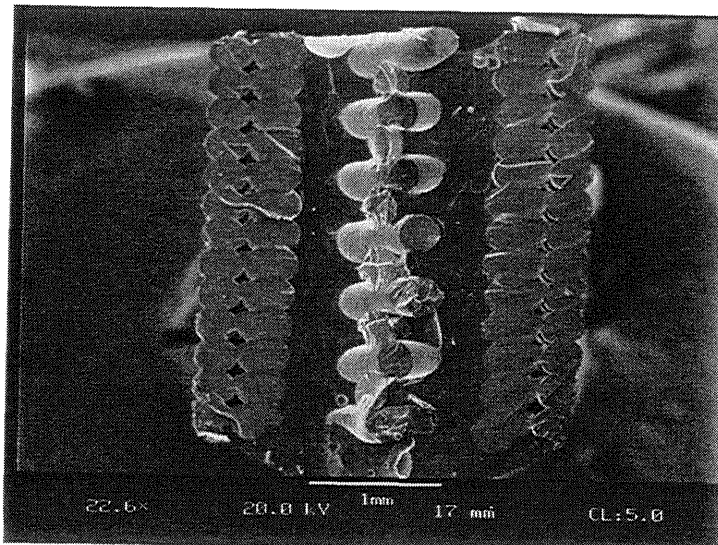
Figure 13: Fracture surface of Clear impregnated sample at 0.02" gap and 27.2X.
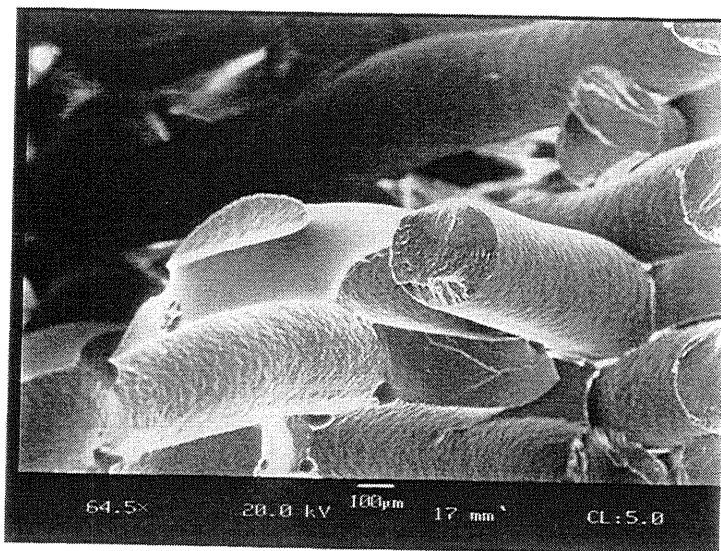
Figure 14: Fracture surface of Clear impregnated sample at 0.02" gap and 64.5X.
Note the pure adhesive failure of the highly ductile matrix.
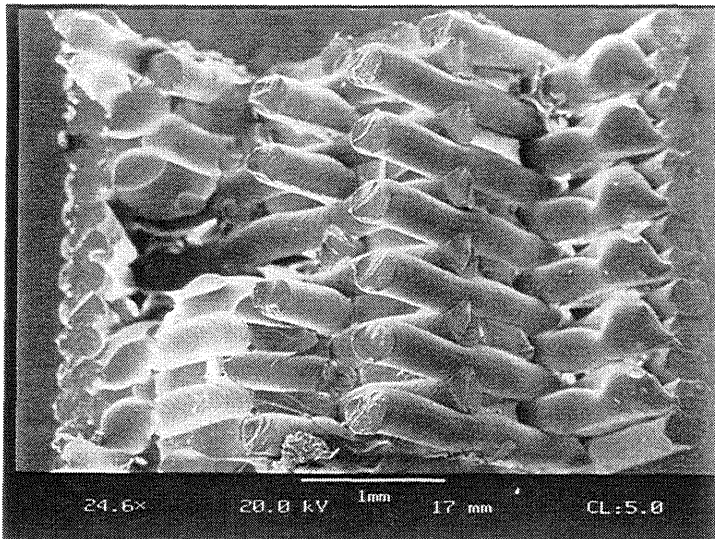
Figure 15: Fracture surface of Clear impregnated sample at 0.03" gap and 24.6X.
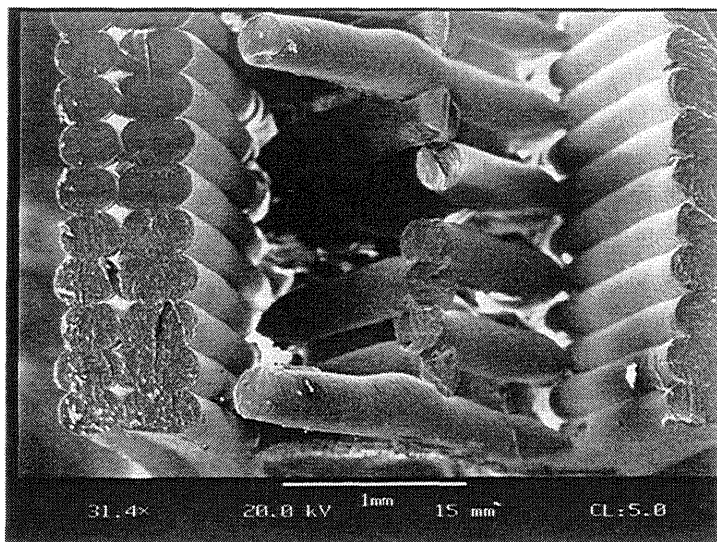
Figure 16: Fracture surface of Clear impregnated sample at 0.05" gap and 31.4X.
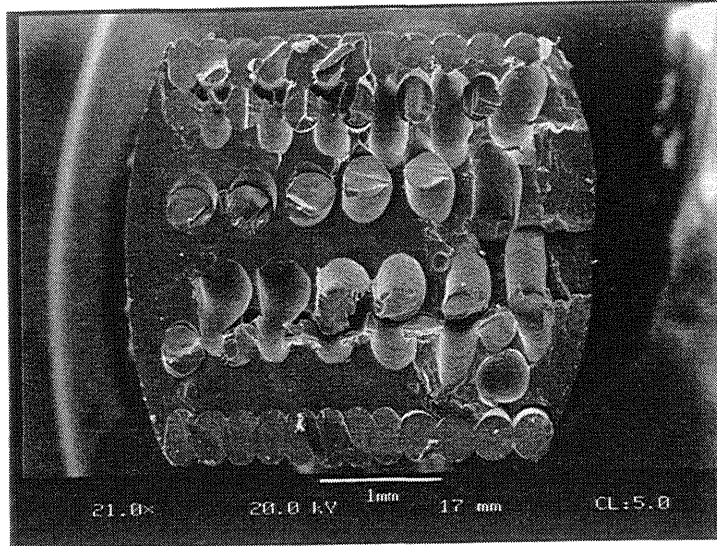
Figure 17: Fracture surface of 5Min impregnated sample at 0.02" gap and 21.0X.

Figure 18: Fracture surface of 5Min impregnated sample at 0.02" gap and 16.1X.
Note the lack of deformation in the adhesive.

435

Figure 19: Fracture surface of 5Min impregnated sample at 0.03" gap and 25.8X.

Figure 20: Fracture surface of 5Min impregnated sample at 0.03" gap and 18.5X.

Figure 21: Fracture surface of 5Min impregnated sample at 0.03" gap and 2100X.
Note the difference in appearance between the ductile failure of the polymer fiber in the upper right as compared to the brittle failure of the matrix in the lower left.
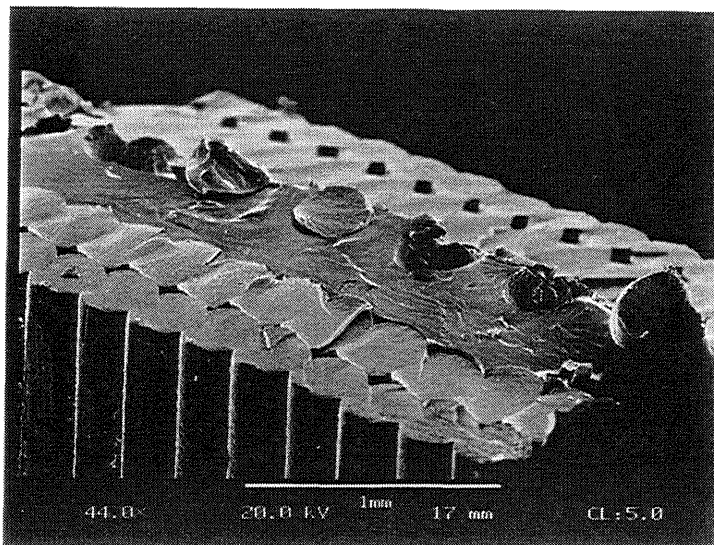

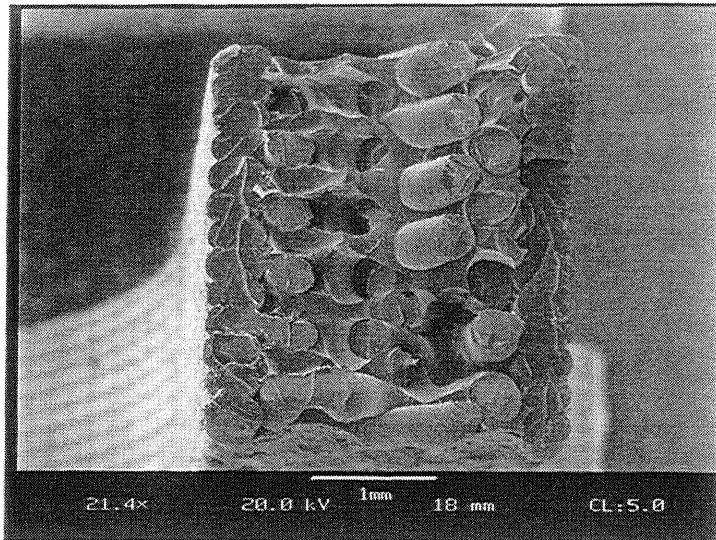Figure 22: Fracture surface of 5Min impregnated sample at 0.05" gap and 22.6X.

437
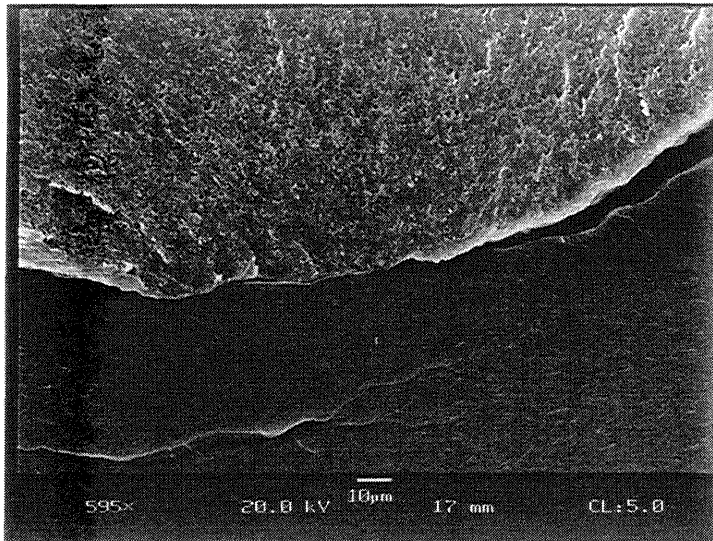
Figure 23: Fracture surface of 5Min impregnated sample at 0.05" gap and 595X.
Note the difference in appearance between the ductile failure of the polymer fiber in
the upper half as compared to the brittle failure of the matrix in the lower.

Figure 24: Fracture surface of 5Min impregnated sample at 0.05" gap and 44X.

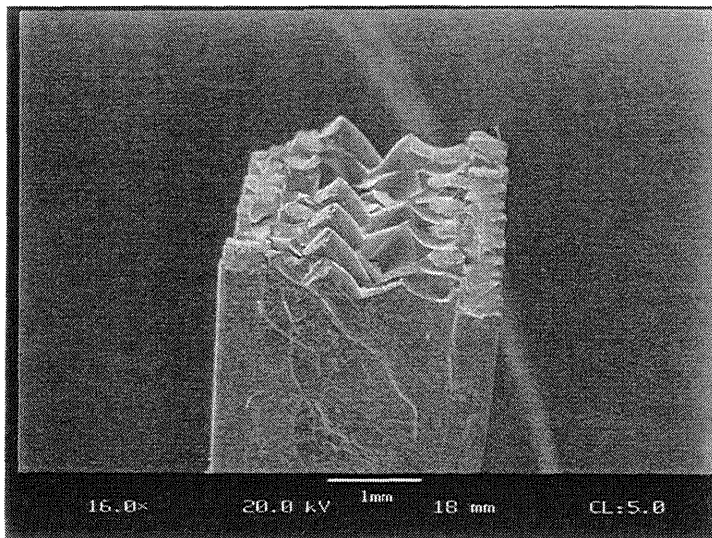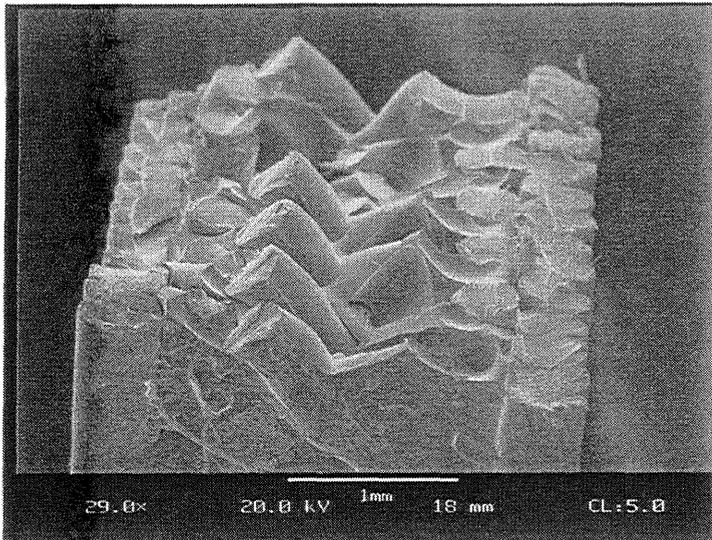Figure 25: Fracture surface of Ultra impregnated sample at 0.02" gap and 21.4X.

Figure 26: Fracture surface of Ultra impregnated sample at 0.02" gap and 16X.

Figure 27: Fracture surface of Ultra impregnated sample at 0.02" gap and 29X.
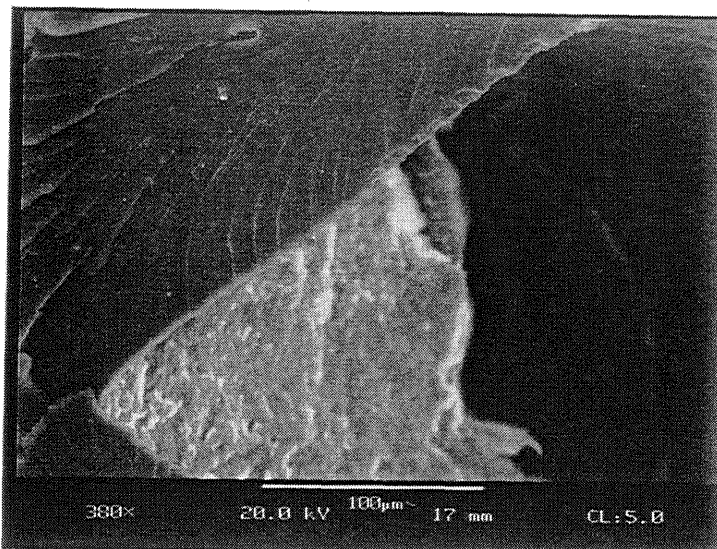

Figure 28: Fracture surface of Ultra impregnated sample at 0.02" gap and 388X.
Note the difference in appearance between the ductile failure of the polymer fiber in
the center of the photomicrograph as compared to the brittle failure of the matrix at
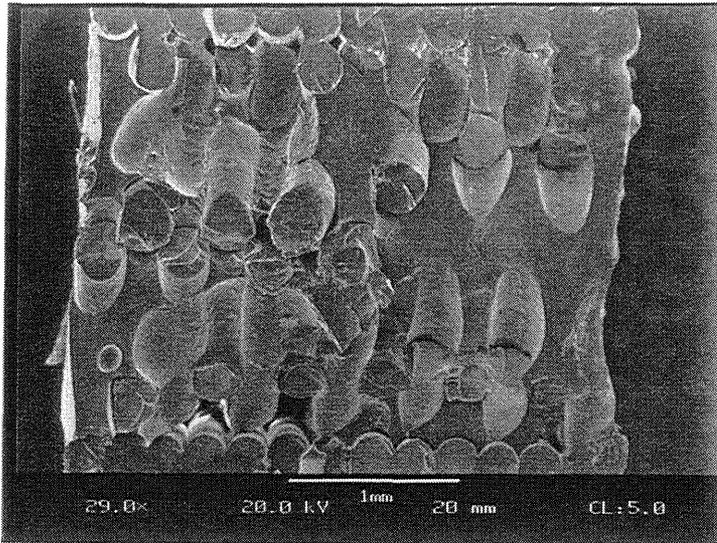the perimeter.

440

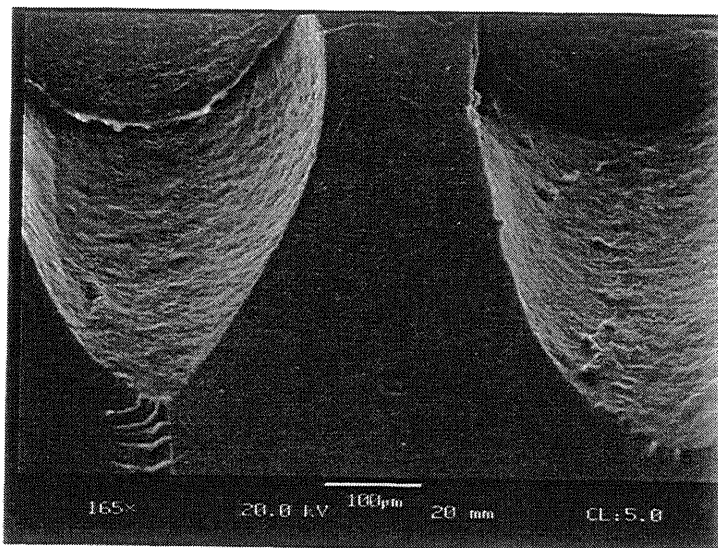Figure 29: Fracture surface of Ultra impregnated sample at 0.03" gap and 29X.

Figure 30: Fracture surface of Ultra impregnated sample at 0.03" gap and 165X.
Note the difference in appearance between the ductile Adhesive failure at the
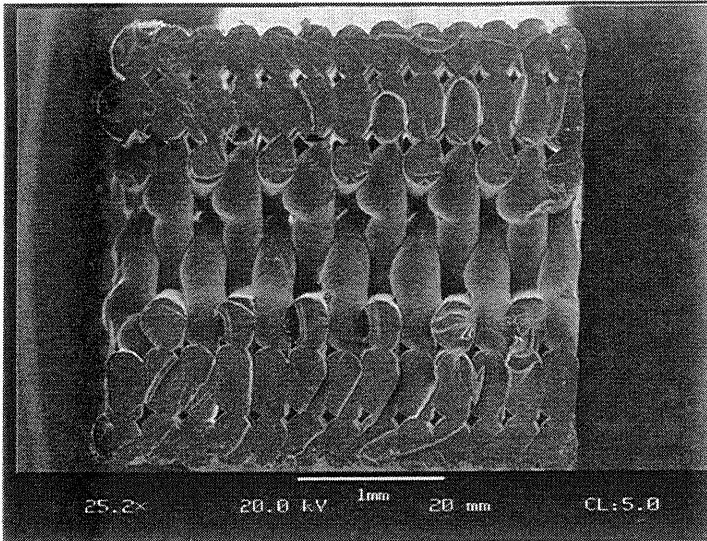fiber/matrix as compared to the brittle failure of the matrix.

441

Figure 31: Fracture surface of Ultra impregnated sample at 0.05" gap and 25.2X.
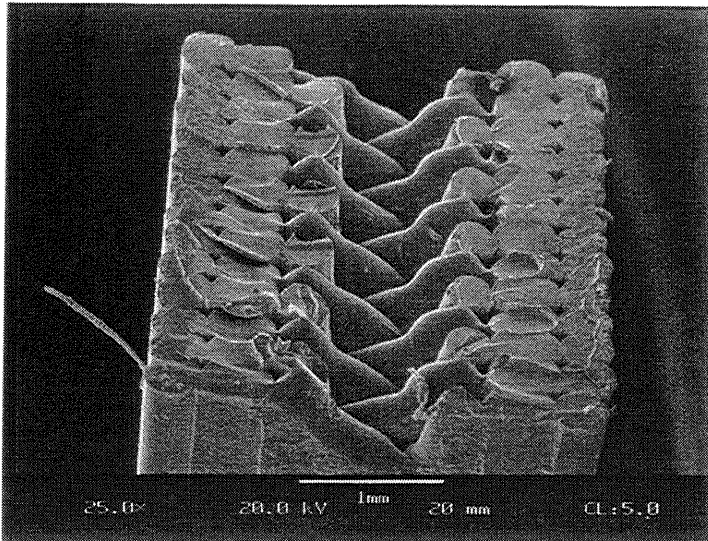Note the lack of deformation in the adhesive.

Figure 32: Fracture surface of Ultra impregnated sample at 0.05" gap and 25X.
Note the lack of deformation in the adhesive.